

Using High-Mass X-ray binaries to probe massive binary evolution: The age distribution of High-Mass X-ray binaries in M33

Kristen Garofali^{1,2}  and Benjamin F. Williams¹

¹Department of Astronomy, University of Washington
Box 351580, U.W., Seattle, WA, USA
emails: garofali@uark.edu, ben@astro.washington.edu

²Department of Physics, University of Arkansas,
825 West Dickson St, Fayetteville, AR, USA
email: garofali@uark.edu

Abstract. High-mass X-ray binaries (HMXBs) provide an exciting window into the underlying processes of both binary as well as massive star evolution. Because HMXBs are systems containing a compact object accreting from a high-mass star at close orbital separations they are also likely progenitors of gamma-ray bursts and gravitational wave sources. We present classification and age measurements for HMXBs in M33 using a combination of deep Chandra X-ray imaging, and archival *Hubble Space Telescope* data. We constrain the ages of the HMXB candidates by fitting the color-magnitude diagrams of the surrounding stars, which yield the star formation histories of the surrounding region. Unlike the age distributions measured for HMXB populations in the Magellanic Clouds, the age distribution for the HMXB population in M33 contains a number of extremely young (<5 Myr) sources. We discuss these results the context of the effect of host galaxy properties on the observed HMXB population.

Keywords. X-rays: binaries, Local Group, stars: imaging

1. Introduction

The majority of massive stars are in close binaries that will interact (e.g. via mass transfer, tides, and common envelope evolution), often dramatically altering the evolution of the component stars (Sana *et al.* 2012; Duchêne & Kraus 2013; Sana *et al.* 2014; Moe & Di Stefano 2017). The evolutionary paths taken depend strongly on often-unknown initial orbital parameters, and suffer from uncertainties in prescriptions for mass loss rates, rotation, metallicity effects, mass transfer efficiency, the common envelope phase, natal kicks, and more (Postnov *et al.* 2006; Dray 2006; Dominik *et al.* 2012; Ivanova *et al.* 2013; Smith 2014; Mandel 2016).

The uncertainties in massive binary evolution can be mitigated by observing and modeling sources at various evolutionary stages. High-mass X-ray binaries (HMXBs), systems containing a compact object (black hole [BH] or neutron star [NS]) and a high-mass ($\gtrsim 10M_{\odot}$) star with close enough orbital separation such that accretion onto the compact object results in an X-ray-bright source, are an intermediate stage of evolution for close binaries with two massive components, and are potential precursors to close compact object binaries, which are sources of gravitational waves and short-duration gamma bursts if the systems merge within a Hubble time (Berger 2014; Belczynski *et al.* 2018).

Thus, HMXBs provide a unique snapshot in time in which to probe massive star and binary evolution, particularly as these relate to close compact object binary formation.

The Local Volume provides an ideal laboratory for studying HMXBs, as they are numerous in star-forming regions and resolvable with *Chandra* at these distances (Mineo *et al.* 2012). Surveys of resolved HMXB populations have probed key questions related to natal kick velocities, X-ray binary (XRB) formation efficiency in different environments, correlations with host galaxy star formation rate (SFR), and the evolutionary status of donor stars (Grimm *et al.* 2003; Coe *et al.* 2005; Antoniou *et al.* 2010; Mineo *et al.* 2012).

Resolved HMXB studies have also revealed subclasses of these binaries, which are typically defined by the spectral type of the donor star (nominally, the secondary in the binary). The most observationally abundant subclass of HMXBs are Be/X-ray binaries (Be-XRBs) (Liu *et al.* 2005; Liu *et al.* 2006), systems that consist of a compact object (most often a NS) accreting material as it passes through the circumstellar disk of an early B star. By contrast, there are fewer known HMXBs with supergiant companions (SG-XRBs), which are typically wind-fed systems, though may also be fed via Roche lobe overflow (RLOF). Still more rarely observed are the subclass of HMXBs that contain a compact object (usually a BH) accreting material from a Wolf-Rayet (WR) star, with only five such systems observed in the Local Volume to date (van Kerkwijk *et al.* 1996; Prestwich *et al.* 2007; Crowther *et al.* 2010; Liu *et al.* 2013; Maccarone *et al.* 2014).

Notably absent from recent HMXB population studies is M33, which is an ideal target as it is close to face-on, and does not suffer from the distance uncertainties and extinction that hamper Galactic samples, and furthermore, as a large star-forming spiral galaxy, probes an environment different from those in the well-studied, but much smaller, Magellanic Clouds (MCs). In addition, M33 has deep coverage from dedicated surveys with *Chandra*, *XMM-Newton* (Tüllmann *et al.* 2011; Williams *et al.* 2015), and the *Hubble Space Telescope* (*HST*), capable of resolving individual HMXBs and their donor stars. Furthermore, recent analysis of X-ray luminosity function (XLF) in M33 reveals a slope consistent with the universal slope expected for a population of HMXBs (Mineo *et al.* 2012), suggestive of a substantial population of HMXBs in the galaxy (Williams *et al.* 2015), of which very few ($\lesssim 5$) have been robustly characterized to date (Long *et al.* 2002; Pietsch *et al.* 2004; Pietsch *et al.* 2006; Orosz *et al.* 2007; Pietsch *et al.* 2009; Trudolyubov 2013).

Herein, we present measurement of the age distribution for new candidate HMXBs in M33. In Section 2 we briefly present the data used as part of this study, along with the source identification and SFH recovery techniques. In Section 3 we present the age distribution for all candidate HMXBs in the sample. Finally, in Section 4 and Section 5 we provide an analysis and discussion of these results in the context of binary evolution, and compact object binaries.

2. Data & Analysis Techniques

In this section, we introduce the catalogs used to find candidate HMXBs in M33, namely *Chandra* imaging from the *Chandra* ACIS Survey of M33 (ChASem33, Tüllmann *et al.* 2011; hereafter T11) for localizing hard X-ray point sources, and archival *HST* data with at least two broad-band filters for selecting optical counterparts to X-ray sources. In addition, we discuss the color magnitude diagram (CMD) fitting technique used to produce spatially resolved SFHs, and thus ages, in the vicinities of candidate HMXBs.

2.1. *Chandra* Catalog

The X-ray sources mined for candidate HMXBs come from the ChASem33 survey (T11), which consists of 662 X-ray sources aligned to the Two Micron All-Sky Survey

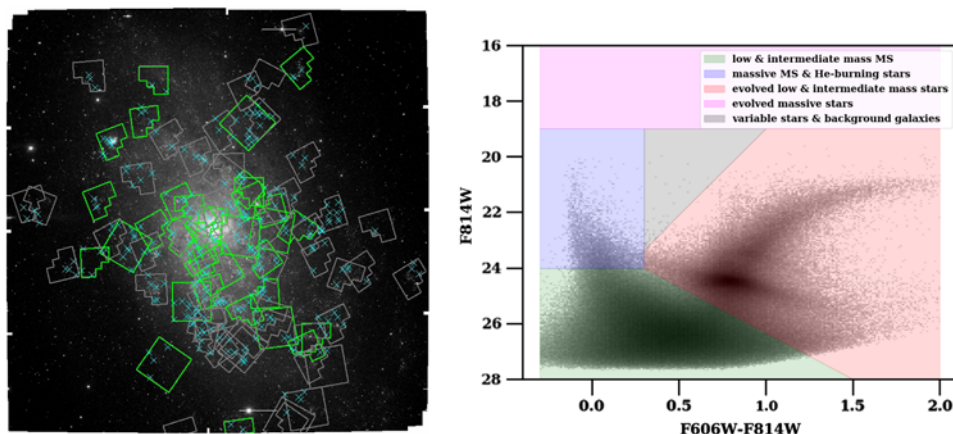


Figure 1. *Left:* R band Local Group Galaxy Survey (Massey *et al.* 2006) image of M33 overlaid with all 89 archival *HST* fields (grey and green), and all 36 fields containing candidate HMXBs (green only). Cyan crosses are X-ray sources from T11 that fall within the current archival *HST* coverage. There are 270 X-ray sources covered by 89 *HST* fields. *Right:* A Hess diagram constructed from all stars in one *HST* field, binned by 0.05 magnitudes in color and magnitude space. The shaded regions delineate sources in different mass ranges and stages of stellar evolution: green: low and intermediate mass main sequence stars; blue: massive main sequence stars (e.g. OB stars) and He-burning stars; red: evolved low and intermediate mass stars (e.g. red giant branch, red clump, and asymptotic giant branch stars); magenta: evolved massive stars (e.g. supergiants); grey: variable stars and background galaxies. Optical counterparts for HMXBs would most likely appear in the blue and magenta shaded regions.

(2MASS) (Cutri *et al.* 2003), and covers $\sim 70\%$ of the D_{25} isophote of M33 down to a limiting 0.35–8.0 keV luminosity of 2.4×10^{34} erg s $^{-1}$ with a total exposure time of 1.4 Ms.

For the purposes of selecting candidate HMXBs we used the X-ray source positions from T11 for pinpointing source locations, in addition to hardness ratios (HRs) and any prior classifications from T11 to narrow down the list of candidate HMXBs. In particular, HRs in the soft (0.35–1.1 keV), medium (1.1–2.6 keV), and hard (2.6–8.0 keV) bands were used for separating soft sources, foreground stars and supernova remnants (SNRs), from harder sources like background active galactic nuclei (AGN) and XRBs, both HMXBs and low-mass X-ray binaries (LMXBs).

2.2. *HST* Photometry & Image Alignment

Optical counterparts to the X-ray sources in T11 were selected using all available archival *HST* photometry in M33 with at least two broad-band filters, totaling 89 unique *HST* fields covering $\sim 40\%$ of the T11 catalog (270 X-ray sources). The archival *HST* coverage of M33, and X-ray point sources from T11 within this coverage are shown in the left panel of Figure 1. Details of the *HST* data reduction, extraction of photometry, and specific fields used in this analysis are presented in Garofali *et al.* (2018).

Identifying *HST* counterparts to X-ray sources in T11 requires precise astrometric alignment to a common frame between data sets. As the T11 catalog is already aligned to 2MASS, we chose to align all archival *HST* fields to 2MASS as well. The alignment procedure coupled with position error from T11 results in X-ray error circles typically $\lesssim 0.7''$ in radius for sources considered here.

With *HST* fields aligned to a common frame as the X-ray data, we can search for optical counterparts to the X-ray sources from T11 with relatively low probabilities of chance coincidences, and thus spurious sources. We inspected all 89 archival *HST* fields

for optical counterparts to X-ray sources, classifying optical counterparts and thus X-ray source types using color and magnitude cuts similar to those depicted in the right panel of Figure 1. We consider a strong candidate HMXB to be a hard X-ray source with an optical counterpart in its error circle that falls in the blue or magenta regions of the Hess diagram in the right panel of Figure 1. Using this criteria, we identify 55 candidate HMXBs, of which we estimate 11 ± 3 may be chance coincidences of OB stars with the X-ray error circle, and thus spurious sources.

2.3. Color-Magnitude Diagram Fitting

We measure ages, or formation timescales for the sample of candidate HMXBs in M33 using the stellar population surrounding each source. Below we briefly detail this process, which first involves selecting the photometric sample in the vicinity of each candidate, and then fitting the stellar photometry using models of stellar evolution.

For young sources ($\lesssim 50$ Myr) such as HMXBs it is possible to determine the age, or formation timescale of the source based on the surrounding stellar population, as most stars are known to form in clusters, and thus in relatively co-eval populations that stay associated in regions of ~ 50 pc on timescales < 60 Myr (Lada & Lada 2003; Gogarten *et al.* 2009; Eldridge *et al.* 2011). Thus, HMXB ages can be measured by performing fits to the CMDs of the surrounding stellar population to produce spatially resolved SFHs.

Because the onset of the HMXB phase may not immediately follow formation of the compact object, there is the possibility that an HMXB which received a strong natal kick when the primary formed a compact object could have moved away from its associated natal stellar population either into isolation, or into a region with a stellar population of unassociated age. However, both theory and observations suggest that very large natal kicks may not be common for HMXBs (Pfahl *et al.* 2002; Coe *et al.* 2005; Sepinsky *et al.* 2005; Linden *et al.* 2009; Coleiro & Chaty 2013). We therefore test stellar population region sizes of 50 pc and 100 pc for measuring SFHs, and find the results to be consistent in both cases. We discuss the results using only the 50 pc regions in Section 3.

To measure the spatially-resolved SFHs in the vicinity of each candidate HMXB, and thus recover ages for each source, we fit the CMDs of the stellar population within 50 pc of the candidate HMXB using the software MATCH (Dolphin 2002), with details of the fitting process and error analysis described in Garofali *et al.* (2018). The resultant SFHs return the SFR in each time bin, which can be used to derive the cumulative distribution of stellar mass formed in the timespan of interest by calculating the total amount of stellar mass formed, and then the associated fraction of the total stellar mass in each time bin. We report both the SFH as well as the cumulative distribution of stellar mass, as the latter can be interpreted as a probability distribution function for the age of the source, with the most likely age represented by the time bin containing the highest fraction of stellar mass formed.

An example of the SFH and associated cumulative stellar mass distribution out to 80 Myr for a candidate HMXB (source 013341.47+303815.9 from T11) is presented in the right and center panels of Figure 2. The most likely age (dotted line) is 7.1 Myr for this source, with the narrowest 68th percentile confidence interval in red. We also display the CMD of the stars within 50 pc of this source in the left panel of Figure 2, with the most likely donor star companion to the HMXB denoted by the cyan star, and Padova group stellar isochrones, consistent with the young age determined from the SFH, overlaid for reference.

3. Results

We identified 55 candidate HMXBs in M33 as hard X-ray point sources associated with potential massive donor star counterparts, the majority ($\sim 80\%$) of which had no classification prior to this work (Grimm *et al.* 2005; T11). The characteristics of each

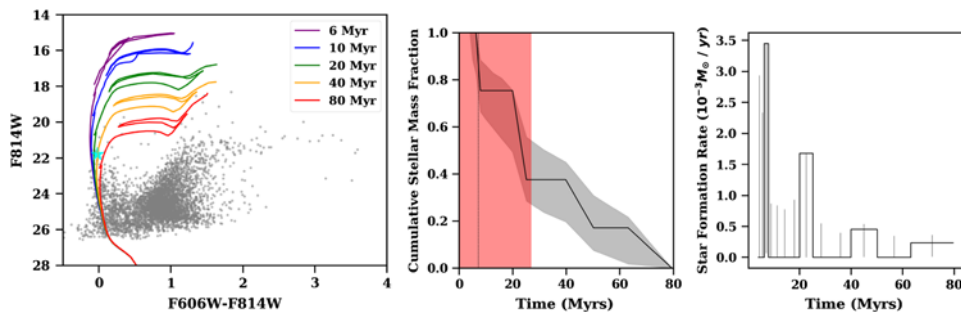


Figure 2. *Left:* The CMD representing the stellar population (grey points) within 50 pc of the HMXB candidate 013341.47+303815.9, with the candidate donor star denoted by the cyan star. Padova group isochrones shifted to the distance and extinction of M33 are overlaid for reference. *Center:* The cumulative stellar mass fraction (black line) formed within 80 Myr post-starburst. The Monte Carlo derived errors on this distribution are in grey, and the most likely age is marked with a dotted line. The narrowest 68th percentile confidence interval on the most likely age is marked in red. *Right:* The corresponding SFH for this candidate HMXB.

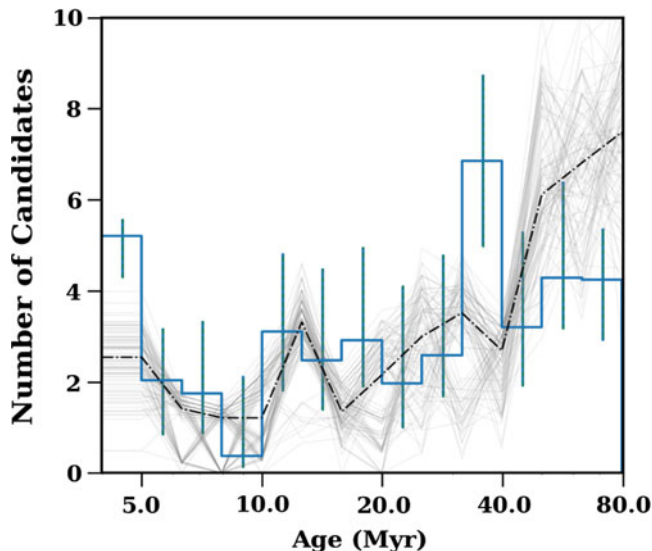


Figure 3. The age distribution calculated using 50 pc regions for all 41 HMXBs in M33 that are in fields sensitive to the MSTO at 80 Myr plotted as a solid blue line. The solid blue histogram represents the number of systems expected in each age bin given the SFHs for all sources. The light grey lines are the control sample: the equivalent age distribution for 100 random draws of 41 non-HMXB X-ray sources in M33, with the median of these 100 draws as a dash-dot line in black.

candidate HMXB are presented in Garofali *et al.* (2018). Here, we describe the age distribution for this population, as measured from the combination of the SFHs for all candidates in the archival *HST* coverage where the imaging was deep enough to be sensitive to the main sequence turn-off at 80 Myr (41 candidate HMXBs).

We built up the age distribution for all candidate HMXBs in fields that passed our depth cuts as the sum of the stellar-mass weighted star formation in each bin, normalized to a total stellar mass formed in 80 Myr for each candidate HMXB of one. This summation yields a distribution that reflects the number of HMXBs expected to form in each time bin. This analysis accounts for the entire SFH for each source, and in this way does not rely on calculating a specific age individual candidate HMXBs.

The HMXB age distribution, built up from the stacked SFHs, is shown in Figure 3 as a solid blue histogram. The light grey lines represent 100 draws of the age distribution for a “control” population, constructed from SFHs in the regions around 41 X-ray sources that are not HMXBs. The median of the 100 realizations is plotted as a dash-dot black line. Compared to the control sample, the age distribution for the candidate HMXBs contains two notable peaks: a young population present at < 5 Myr post-starburst, and a delayed population appearing at 40 Myr post-starburst. In Section 4 and Section 5 we discuss these two populations in the context of binary evolution, and compact object binaries.

4. Discussion

In this section we discuss how the host galaxy environment affects HMXB formation efficiency, and how the age distribution for HMXBs in M33 relates to different HMXB subpopulations.

4.1. Age Distribution and Environment

The age distribution for HMXBs has been measured from spatially-resolved SFHs in a number of other nearby galaxies, finding similar preference for HMXB formation ~ 40 Myr post-starburst in the Small Magellanic Cloud (SMC), NGC 300 and NGC 2403 (Antoniou *et al.* 2010; Williams *et al.* 2013), and 6-25 Myr post-starburst in the Large Magellanic Cloud (LMC) (Antoniou & Zezas 2016). These differing timescales for formation can stem both from differences in the host environment, as well as point to distinct HMXB subpopulations. We discuss the former here in terms of the effects of metallicity, and the latter in the following section in terms of binary evolution.

Metallicity may play a role in HMXB formation efficiency via its effect on the line-driven winds of massive stars, which may affect HMXB evolution via mass loss and orbital evolution through loss of angular momentum (Dray 2006; Linden *et al.* 2010). Because M33 has a measured metallicity gradient, from solar in the interior 3 kpc to LMC-like beyond 3 kpc (Magrini *et al.* 2007), we tested for any metallicity dependence in the HMXB subpopulations by constructing the age distribution separately for sources with galactocentric radii < 3 kpc, and those with radii > 3 kpc. We find that the small number of sources outside 3 kpc prohibits any definitive statement on the differences between HMXB populations in M33 at solar versus LMC metallicities. However, we do note that the very young sources (< 5 Myr) are found throughout the galaxy, and therefore don’t appear to be a strongly metallicity dependent population, at least above the threshold metallicity that is roughly LMC-like.

4.2. Age Distribution and Binary Evolution

The age distribution for HMXBs in M33 has distinct peaks at very young ages (< 5 Myr), and intermediate ages (~ 40 Myr). Below, we discuss these features in the context of HMXB subpopulations and binary evolution.

4.2.1. Early Onset HMXBs: SG-XRBs with Massive Compact Objects?

The formation and appearance of candidate HMXBs < 5 Myr post-starburst in M33 implies a population of massive progenitors ($\gtrsim 40 M_{\odot}$) with the potential for forming massive BHs (Fryer *et al.* 2012). Indeed binary population synthesis simulations predict formation of a population of BHs accreting material from the winds of their supergiant companions < 10 Myr after a burst of star formation (Linden *et al.* 2009). However mass thresholds for BH formation often rely on models of single star evolution. Binary evolution

processes, such as mass transfer and envelope stripping, allow for formation of NS relatively rapidly post-starburst (~ 5 Myr), and therefore from very massive progenitors, at least some small fraction of the time (Belczynski & Taam 2008). Thus very young ages, as measured here for a subsample of candidate HMXBs in M33, do not definitively point to a population of BHs. The only source in this young subpopulation for which the compact object has been independently confirmed to be a BH is M33 X-7 (Orosz *et al.* 2007).

We can also infer HMXB characteristics by analyzing the candidate donor star photometry. In particular, if models suggest that young systems are likely SG-XRBs hosting BHs then we may expect the observed young candidate HMXBs in M33 to have the brightest donor star counterparts in the sample. In fact, for most of these young sources the *HST* colors and magnitudes for the likely donor stars are not bright enough to be indicative of supergiants. The relatively faint photometry of the optical counterparts for these young candidate HMXBs coupled with rapid formation timescales measured from SFHs suggests that these systems either have B type donor stars coupled with initially very massive primaries, that the unexpected secondary star photometry is a signature of binary evolution, or that these systems were actually formed at later times. We expound upon each of these possibilities below.

Current models of binary evolution predict that Be-BH XRBs should be rare, as the high mass ratio between the very massive primary needed to form a BH and the B star secondary will often result in a common envelope merger (Belczynski & Ziolkowski 2009). As there is only one known Be-BH binary in the Milky Way (Casares *et al.* 2014; Ribó *et al.* 2017), it seems unlikely there would be multiple such sources in M33, i.e. B star secondaries coupled with much more massive primaries. Instead of originating from systems with steep mass ratios, these young candidate HMXBs may have donor stars that due to binary evolution processes only appear under-massive. This is difficult to quantify, however, as the expected photometry of the counterpart given past history of binary interactions (e.g. mass transfer, common envelope evolution, spin-up, etc.) is difficult to constrain without knowledge of the initial binary parameters and detailed modeling. Finally, it is instead possible that these candidate HMXBs are not as young as the *most likely* age from the SFH suggests. In particular, for sources lying in regions with multiple bursts of star formation we can only quantify the probability that a source formed at a particular time, and in fact the young candidate HMXBs discussed here all have non-zero probability of forming at later times post-starburst, consistent with fainter donor stars.

The uncertainty regarding the relationship between system age and system components discussed here highlights the need for follow-up, both spectroscopically to determine donor star type, and also via novel methods for discerning compact object type and mass. In the absence of dynamical mass measurements for a large number of sources, *NuSTAR* observations of bright candidate HMXBs in M33 may help determine compact object type (Lazzarini *et al.* 2018).

4.2.2. Delayed Onset HMXBs: Be-XRBs

The peak in HMXB formation efficiency around 40 Myr has previously been ascribed to Be-XRBs (Linden *et al.* 2009; Antoniou *et al.* 2010; Williams *et al.* 2013), as these systems should form efficiently on these timescales given considerations of the IMF and binary evolution.

Under the assumption of a Kroupa IMF and a minimum mass threshold for compact object formation, there will be more NS that form from systems right at the minimum mass threshold than NS forming from progenitors more massive than this. Theory and observation suggest this minimum mass for NS formation is $\sim 8 M_{\odot}$, which corresponds

to ~ 40 Myr stellar lifetime, and thus the formation of the largest number of NS on this timescale. In addition, the Be phenomenon, i.e. B star mass loss activity, has been shown observationally to peak between ~ 25 -80 Myr, implying that the Be phenomenon itself may be the product of binary evolution (McSwain & Gies 2005), namely B star secondaries spun up by mass transfer in a binary on these timescales.

The donor star photometry for the candidate HMXBs contributing to the 40 Myr peak in the age distribution in M33 is compatible with this picture, with colors and magnitudes consistent with B stars. Spectroscopic follow-up is still needed to determine which systems actually contain Be stars, which will also cull the sample for X-ray follow-up to determine which systems host NS compact objects.

5. Implications

The primary features of the candidate HMXB age distribution in M33, namely peaks in HMXB formation efficiency at < 5 Myr and ~ 40 Myr post-starburst, are indicative of HMXB subpopulations, possibly SG-XRBs hosting BHs and Be-XRBs hosting NS, respectively. As HMXBs are ostensibly products of binary evolution that have remained bound following the death of the primary, studying the past and future evolution of these systems can be an important tool for understanding the binary evolution pathways that lead to compact object binaries, and possibly compact object mergers. Below, we discuss the observed subpopulations of HMXBs in M33 and their implications for compact object binaries and gravitational wave sources.

Young HMXBs are more likely to host BHs as compact objects, but understanding their future evolution and ultimate fate in the context of gravitational wave sources requires a detailed characterization of the system components. The only young HMXB in M33 for which this kind of characterization has been done is M33 X-7, which, with a $\sim 15.65 M_{\odot}$ BH and a $\sim 70 M_{\odot}$ donor star secondary, has the possibility to form a BH-BH binary if it survives common envelope evolution and avoids a merger. Even so, systems like this are clearly incapable of being precursors to some of the more massive BH-BH mergers observed by LIGO, which are more likely to originate from systems like WR-XRBs. However, young SG-XRBs with the right orbital configuration may be capable of forming BH-NS binary mergers, for which the merger rate densities are not yet constrained by LIGO.

The prevalence of Be-XRBs on ~ 40 Myr timescales in M33 and other Local Group populations may be informative regarding preferred evolution channels for efficiently forming the precursors to NS-NS binaries. The appearance of Be-XRBs on these timescales requires that the binary survives the death throes of the primary, which may preferentially occur if the primary undergoes an electron capture supernova that imparts a smaller kick to the system (Linden *et al.* 2009). The efficiency with which this supernova mechanism operates to produce bound binaries, and the particular timescale on which it functions may be a function of metallicity (Podsiadlowski *et al.* 2004), though observational studies in the Local Group demonstrate that Be-XRBs form efficiently between ~ 25 -60 Myr across a range of metallicities from sub-solar to solar. If such Be-XRBs survive the future evolution of the Be star secondary, this implies an efficient pathway for forming close NS-NS binaries, and therefore possible NS-NS mergers in a range of environments (Tauris *et al.* 2017).

Leveraging HMXBs as probes of binary evolution, and using them to understand the pathways that lead to compact object mergers requires close feedback between theory and observations. In particular, full characterization of an HMXB, from primary and secondary star properties to orbital characteristics, provides constraints for models of binary evolution by requiring the model prescriptions for common envelope evolution,

mass transfer, natal kicks, and more to effectively reproduce the observed system parameters. Likewise, well-tested models of binary evolution can be used to evolve HMXBs forward in time to better understand their connection to close compact object binary populations. The sample of candidate HMXBs in M33 and their measured age distribution discussed here provides a population ripe for follow-up to continue illuminating the connections between HMXBs and compact object mergers.

References

- Antoniou, V., & Zezas, A. 2016, *MNRAS*, 459, 528
- Antoniou, V., Zezas, A., Hatzidimitriou, D., & Kalogera, V. 2010, *ApJ*, 716, L140
- Belczynski, K., & Taam, R. E. 2008, *ApJ*, 685, 400
- Belczynski, K., & Ziolkowski, J. 2009, *ApJ*, 707, 870
- Belczynski, K., Askar, A., Arca-Sedda, M., *et al.* 2018, *A&A*, 615, A91
- Berger, E. 2014, *ARA&A*, 52, 43
- Berghea, C. T., Dudik, R. P., Tincher, J., & Winter, L. M. 2013, *ApJ*, 776, 100
- Binder, B., Williams, B. F., Kong, A. K. H., *et al.* 2016, *MNRAS*, 457, 1636
- Casares, J., Negueruela, I., Ribó, M., *et al.* 2014, *Nature*, 505, 378
- Coe, M. J., Edge, W. R. T., Galache, J. L., & McBride, V. A. 2005, *MNRAS*, 356, 502
- Coleiro, A., & Chaty, S. 2013, *ApJ*, 764, 185
- Crowther, P. A., Barnard, R., Carpano, S., *et al.* 2010, *MNRAS*, 403, L41
- Cutri, R. M., Skrutskie, M. F., van Dyk, S., *et al.* 2003, 2MASS All Sky Catalog of point sources.
- . 2002, *MNRAS*, 332, 91
- Dominik, M., Belczynski, K., Fryer, C., *et al.* 2012, *ApJ*, 759, 52
- Dray, L. M. 2006, *MNRAS*, 370, 2079
- Duchêne, G., & Kraus, A. 2013, *ARA&A*, 51, 269
- Eldridge, J. J., Langer, N., & Tout, C. A. 2011, *MNRAS*, 414, 3501
- Fryer, C. L., Belczynski, K., Wiktorowicz, G., *et al.* 2012, *ApJ*, 749, 91
- Garofali, K., Williams, B. F., Hillis, T., *et al.* 2018, *MNRAS*, 479, 3526
- Gogarten, S. M., Dalcanton, J. J., Williams, B. F., *et al.* 2009, *ApJ*, 691, 115
- Grimm, H.-J., Gilfanov, M., & Sunyaev, R. 2003, *MNRAS*, 339, 793
- Grimm, H.-J., McDowell, J., Zezas, A., Kim, D.-W., & Fabbiano, G. 2005, *ApJS*, 161, 271
- Ivanova, N., Justham, S., Chen, X., *et al.* 2013, *A&A Rev.*, 21, 59
- Jennings, Z. G., Williams, B. F., Murphy, J. W., *et al.* 2012, *ApJ*, 761, 26
- . 2014, *ApJ*, 795, 170
- Lada, C. J., & Lada, E. A. 2003, *ARA&A*, 41, 57
- Lazzarini, M., Hornschemeier, A. E., Williams, B. F., *et al.* 2018, *ApJ*, 862, 28
- Linden, T., Kalogera, V., Sepinsky, J. F., *et al.* 2010, *ApJ*, 725, 1984
- Linden, T., Sepinsky, J. F., Kalogera, V., & Belczynski, K. 2009, *ApJ*, 699, 1573
- Liu, J.-F., Bregman, J. N., Bai, Y., Justham, S., & Crowther, P. 2013, *Nature*, 503, 500
- Liu, Q. Z., van Paradijs, J., & van den Heuvel, E. P. J. 2005, *A&A*, 442, 1135
- . 2006, *A&A*, 455, 1165
- Long, K. S., Charles, P. A., & Dubus, G. 2002, *ApJ*, 569, 204
- Maccarone, T. J., Lehmer, B. D., Leyder, J. C., *et al.* 2014, *MNRAS*, 439, 3064
- Magrini, L., Vílchez, J. M., Mampaso, A., Corradi, R. L. M., & Leisy, P. 2007, *A&A*, 470, 865
- Mandel, I. 2016, *MNRAS*, 456, 578
- Massey, P., Olsen, K. A. G., Hodge, P. W., *et al.* 2006, *AJ*, 131, 2478
- McSwain, M. V., & Gies, D. R. 2005, *ApJS*, 161, 118
- Mineo, S., Gilfanov, M., & Sunyaev, R. 2012, *MNRAS*, 419, 2095
- Moe, M., & Di Stefano, R. 2017, *ApJS*, 230, 15
- Orosz, J. A., McClintock, J. E., Narayan, R., *et al.* 2007, *Nature*, 449, 872
- Pfahl, E., Rappaport, S., Podsiadlowski, P., & Spruit, H. 2002, *ApJ*, 574, 364
- Pietsch, W., Haberl, F., Sasaki, M., *et al.* 2006, *ApJ*, 646, 420
- Pietsch, W., Mochejska, B. J., Misanovic, Z., *et al.* 2004, *A&A*, 413, 879
- Pietsch, W., Haberl, F., Gaetz, T. J., *et al.* 2009, *ApJ*, 694, 449

- Podsiadlowski, P., Langer, N., Poelarends, A. J. T., *et al.* 2004, *ApJ*, 612, 1044
- Postnov, K. A., & Yungelson, L. R. 2006, *Living Reviews in Relativity*, 9, 6
- Poutanen, J., Fabrika, S., Valeev, A. F., Sholukhova, O., & Greiner, J. 2013, *MNRAS*, 432, 506
- Prestwich, A. H., Kilgard, R., Crowther, P. A., *et al.* 2007, *ApJ*, 669, L21
- Ribó, M., Munar-Adrover, P., Paredes, J. M., *et al.* 2017, *ApJ*, 835, L33
- Rizzi, L., Tully, R. B., Makarov, D., *et al.* 2007, *ApJ*, 661, 815
- Sana, H., de Mink, S. E., de Koter, A., *et al.* 2012, *Science*, 337, 444
- Sana, H., Le Bouquin, J.-B., Lacour, S., *et al.* 2014, *ApJS*, 215, 15
- Sepinsky, J., Kalogera, V., & Belczynski, K. 2005, *ApJ*, 621, L37
- Smith, N. 2014, *ARA&A*, 52, 487
- Tauris, T. M., Kramer, M., Freire, P. C. C., *et al.* 2017, *ApJ*, 846, 170
- Trudolyubov, S. P. 2013, *MNRAS*, 435, 3326
- Tüllmann, R., Gaetz, T. J., Plucinsky, P. P., *et al.* 2011, *ApJS*, 193, 31
- van Kerkwijk, M. H., Geballe, T. R., King, D. L., van der Klis, M., & van Paradijs, J. 1996, *A&A*, 314, 521
- Williams, B. F., Binder, B. A., Dalcanton, J. J., Eracleous, M., & Dolphin, A. 2013, *ApJ*, 772, 12
- Williams, B. F., Hatzidimitriou, D., Green, J., *et al.* 2014, *MNRAS*, 443, 2499
- Williams, B. F., Wold, B., Haberl, F., *et al.* 2015, *ApJS*, 218, 9
- Williams, B. F., Lazzarini, M., Plucinsky, P., *et al.* 2018, ArXiv e-prints, [arXiv:1808.10487](https://arxiv.org/abs/1808.10487)

Discussion

FRAGOS: Orbital periods are important constraints for determining the evolutionary history of an XRB. What is the prospect of measuring orbital periods for some of the HMXBs with identified companions?

GAROFALI: Many of the donor star companions identified in M33 are faint (22nd-24th magnitude), so a 10-meter class telescope such as Keck would be needed to first confirm companions spectroscopically, and then follow-up with dedicated radial velocity monitoring. For the smaller number of sources with companions brighter than 22nd magnitude, spectroscopic monitoring to determine donor star spectral class and orbital period would be possible with an 8-meter telescope like Gemini. The first step should be spectroscopic follow-up for the strongest candidate HMXBs to further cull the list down to the best sources for more time-intensive radial velocity monitoring to measure orbital periods.